AIP Advances

Encapsulation and substitution of Fe in C12A7 ($12CaO \cdot 7Al_2O_3$)

Cite as: AIP Advances **10**, 015242 (2020); https://doi.org/10.1063/1.5140678
Submitted: 29 November 2019 . Accepted: 09 January 2020 . Published Online: 27 January 2020

Navaratnarajah Kuganathan, Evangelos Gkanas, and Alexander Chroneos

Encapsulation and substitution of Fe in C12A7 ($12CaO{\cdot}7Al_2O_3$)

Cite as: AIP Advances 10, 015242 (2020); doi: 10.1063/1.5140678
Submitted: 29 November 2019 • Accepted: 9 January 2020 •
Published Online: 27 January 2020

View Online Export Citation CrossMark

Navaratnarajah Kuganathan,[1,2,a] Evangelos Gkanas,[3,4] and Alexander Chroneos[1,2]

AFFILIATIONS

[1] Department of Materials, Imperial College London, London SW7 2AZ, United Kingdom
[2] Faculty of Engineering, Environment and Computing, Coventry University, Priory Street, Coventry CV1 5FB, United Kingdom
[3] Hydrogen for Mobility Lab, Materials and Processes for Energy Needs Research Group, Institute for Future Transport and Cities, Coventry University, Priory Street, Coventry CV1 5FB, United Kingdom
[4] National Centre for Scientific Research Demokritos, 15341 Agia Paraskevi, Attica, Greece

[a] **Author to whom correspondence should be addressed:** n.kuganathan@imperial.ac.uk

ABSTRACT

Framework modification by doping of Fe^{3+} ions in C12A7 has been recently considered for tailoring its thermal, electronic, and optical properties. Here, we use density functional theory calculations to predict the thermodynamical stability and electronic structures of a single Fe atom encapsulated and substituted by both stoichiometric and electride forms of C12A7. In both forms, exoergic encapsulation is observed, and the resultant complexes exhibit magnetic behavior inferring that they are promising magnetic material candidates for spintronic devices. While the electride form of C12A7 transfers 0.86*e* to Fe, only a small amount of charge (0.14*e*) is transferred from Fe to the cages in the stoichiometric form. Substitution of Fe for Al in both forms of C12A7 is endoergic, and the electride form is more favorable by 1.60 eV than the stoichiometric form. Both encapsulation and substitution introduce Fe sub-bands between the top of the valence band and the Fermi energy level, featuring them as promising materials in catalysis, optics, and electronics.

I. INTRODUCTION

Rapid advancement of electronic applications necessitates the development of new oxide materials that are cheap and non-toxic and have tunable characteristics. Dodecacalcium hepta-aluminate (C12A7) is an inorganic nanoporous oxide, and it has attracted attention recently for many useful research activities due to many reasons including its non-toxicity, chemical stability, low cost, and unit cell containing 12 cages.[1–6] The chemical formula of stoichiometric C12A7 is represented as $[Ca_{24}Al_{28}O_{64}]^{4+}{\cdot}(O^{2-})_2$ [C12A7:O^{2-}], where two O^{2-} ions compensate the positively charged framework and occupy two out of 12 cages. These two O^{2-} ions are called extra-framework oxygen ions. The inner diameter of its cage is ~0.4 nm, and there is an opening between two adjacent cages with a diameter of ~0.1 nm.[2] A range of atoms and ions have been encapsulated to replace extra-frame oxygen ions partially or fully.[6–16] In particular, when both O^{2-} ions are replaced by four electrons, the stoichiometric form is transferred to the electride form $[Ca_{24}Al_{28}O_{64}]^{4+}{\cdot}(e^-)_4$ [C12A7:e^-].[4]

Many experimental and theoretical works have been reported on the encapsulation or doping of anions. However, very few studies on the doping of framework cations (Ca^{2+} and Al^{3+}) in C12A7:O^{2-} are available in the literature.[17–21] Co-doping of Zn and P on the Al site resulted in a reduction in the ionic conductivity compared to that determined in the undoped C12A7.[22] In a study by Bertoni *et al.*,[17] a similar observation was noted for the doping of Mg^{2+} on the Ca site. Si-doped C12A7:O^{2-} has been considered as a catalyst for the decomposition of hydrocarbon by Hayashi *et al.*[23] The experimental study by Palacios *et al.*[20] showed that Ga substitution on the Al site introduces an expansion in the unit cell. Density functional theory (DFT) simulations were performed by Huang *et al.*[24] to modify the framework of C12A7 by doping cations with +2, +3, +4, and +5 charges and examine the impact on the structural and electronic properties.

Ebbinghaus *et al.*[21] recently reported the synthesis of 1% mol Fe substituted on the Al site in C12A7:O^{2-} using the floating zone method and observed the expansion of the lattice parameter by ~0.002 Å. Their study also confirmed the tetrahedral coordination of Fe with the +3 oxidation state. The resultant compound exhibited magnetic moment, and the oxygen diffusion had been lowered due to the strong binding nature of cage wall oxygen with Fe. Recently, Ruttanapun *et al.*[25] calculated the optical gap and thermal conductivity of Fe-doped C12A7:O^{2-} and concluded that both properties were influenced by the Fe substitution. Physical properties of Fe-doped C12A7:O^{2-} have been studied. However, its thermodynamical stability and chemical properties have not been explored yet. Furthermore, the electride form of C12A7 (C12A7:e^-) is also interesting to be considered for doping, and this study was not considered experimentally yet. Although a previous simulation[24] considered the doping of cations including Fe in both forms of C12A7, full analysis is only available for Cu, Ir, P, and V. Furthermore, the encapsulation of Fe is also important to be considered. Theoretical simulations based on the DFT are useful to examine the chemical nature of Fe-doped and/or encapsulated C12A7, charge on the Fe atom, magnetic moment of the resultant complex, and electronic structure with charge density associated with the dopant. Dispersion forces are also important for the system containing free-electrons. Current DFT methods have the ability to calculate this additional attractive energy term arising from dispersion.

In this study, spin-polarized mode DFT together with dispersion correction is used to calculate the structures of a single Fe atom encapsulated in one of the empty cages and substituted on the Al site in both stoichiometric and electride forms of C12A7. Simulations enabled us to calculate the incorporation and substitution energies, optimized structures, charge on the Fe atom, magnetic moment of the undoped and doped structures, and electronic structures together with charge densities.

II. COMPUTATIONAL METHODS

All calculations were performed using a DFT code VASP (Vienna *Ab initio* Simulation Program).[26,27] This code uses projected augmented wave (PAW) potentials.[28] Exchange-correlation was modeled using generalized gradient approximation (GGA) with the Perdew, Burke, and Ernzerhof (PBE)[29] function as implemented in the VASP code. A cubic lattice containing two molecules of $12CaO{\cdot}7Al_2O_3$ with a lattice constant of 11.98 Å was used in all calculations. A plane-wave basis set with a cut-off of 500 eV and a 2 × 2 × 2 Monkhorst-Pack *k*-point mesh[30] yielding 8 *k* points were used. Atomic positions were relaxed using the conjugate gradient algorithm[31] until the forces acting on the atoms were smaller than 0.001 eV/Å. Dispersion was included in the form of pairwise force field parameterized by Grimme *et al.*[32] in the VASP code. Bader charge analysis[33] was carried out to calculate the charge on the encapsulated and substituted Fe atom in both forms of C12A7.

Encapsulation energy for a single Fe atom in C12A7:O^{2-} was calculated using the following equation:

$$E_{enc} = E_{(\mathrm{Fe:C12A7:O^{2-}})} - E_{(\mathrm{C12A7:O^{2-}})} - E_{(\mathrm{Fe})}, \quad (1)$$

where $E_{(\mathrm{Fe:C12A7:O^{2-}})}$ is the total energy of an Fe atom encapsulated in C12A7:O^{2-}, $E_{(\mathrm{C12A7:O^{2-}})}$ is the total energy of bulk C12A7:O^{2-}, and $E_{(\mathrm{Fe})}$ is the energy of a single Fe atom.

Substitution energy for a single Fe atom to replace a single Al atom in the C12A7:O^{2-} was calculated using the following equation:

$$E_{sub} = E_{(\mathrm{Fe.C12A7:O^{2-}})} + E_{(\mathrm{Al})} - E_{(\mathrm{C12A7:O^{2-}})} - E_{(\mathrm{Fe})}, \quad (2)$$

where $E_{(\mathrm{Fe.C12A7:O^{2-}})}$ is the total energy of an Fe atom substituted on the Al site in C12A7:O^{2-}, $E_{(\mathrm{C12A7:O^{2-}})}$ is the total energy of bulk C12A7:O^{2-}, and $E_{(\mathrm{Fe})}$ and $E_{(\mathrm{Al})}$ are the total energies of a single Fe atom and a single Al atom, respectively.

III. RESULTS AND DISCUSSION

A. Structure and electronic properties of C12A7

C12A7 exhibits a cubic structure with a space group of $I\bar{4}3d$.[1] Its experimentally observed lattice parameters are a = b = c = 11.99 Å and α = β = γ = 90°.[1] Both C12A7:O^{2-} and C12A7:e^- bulk structures were optimized under constant pressure to calculate their equilibrium lattice constants. Figure 1 shows the optimized structures and cages occupied with extra-framework oxygen and electrons. The calculated lattice parameters for C12A7:O^{2-} (a = 12.05 Å, b = c = 12.01 Å, α = 90.02°, β = 89.95°, and γ = 89.93°) are in good agreement with the experiment.[1] There is a slight distortion observed in the lattice constants and angles due to the electrostatic attraction formed between the cage pole Ca^{2+} ions and extra-framework O^{2-} ions, as shown in Fig. 1(b). The cage pole distance (4.21 Å) is ~1.50 Å shorter than that calculated in an empty cage. In the case of C12A7:e^- bulk, there is a slight elongation in the lattice constants (a = b = c = 12.06 Å and α = β = γ = 90°), but the relaxed structure maintains its cubic form.

Calculated electronic properties of both C12A7:O^{2-} and C12A7:e^- have been discussed in previous studies.[13,14,16,34] C12A7:O^{2-} is an insulator, and C12A7:e^- is metallic [refer to DOS plots in

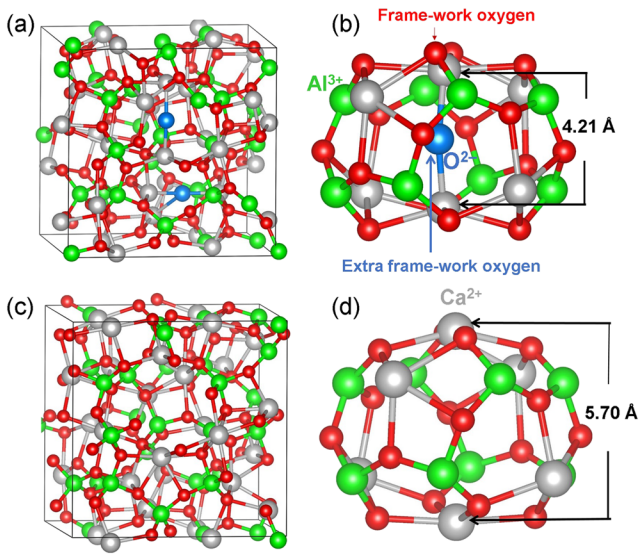

FIG. 1. Relaxed structures of (a) C12A7:O^{2-} bulk, (b) a cage showing the occupation of extra-framework O^{2-} ion in C12A7:O^2, (c) C12A7:e^- bulk, and (d) a cage occupied with 1/3e^- in C12A7:e^-

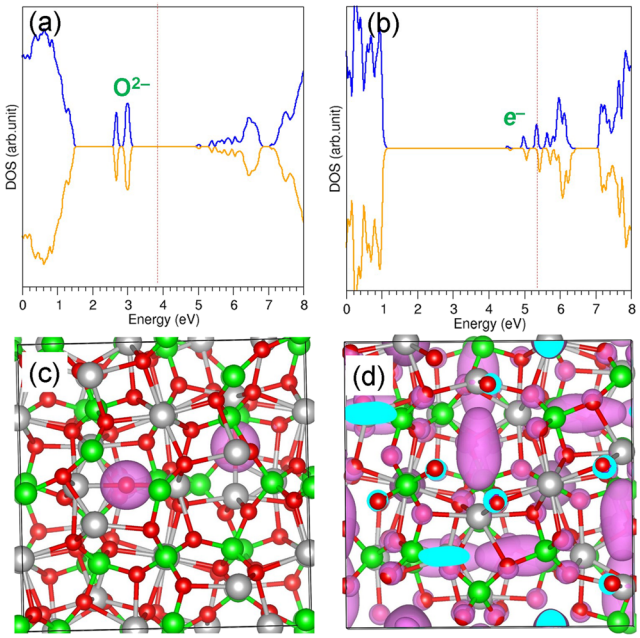

FIG. 2. DOS plots of (a) C12A7:O^{2-} bulk and (b) C12A7:e^- bulk and constant charge density plots associated with (c) the extra-framework O^{2-} ion in C12A7:O^{2-} and (d) electrons in C12A7:e^-.

Figs. 2(a) and 2(b)]. The metallic nature of C12A7:e^- is due to the delocalized extra-framework electrons in the lattice [refer to Fig. 2(d)]. Peaks associated with the extra-framework O^{2-} ions (between 2.50 eV and 3.00 eV) in C12A7:O^{2-} are slightly further away from the valence bands, and these peaks correspond to the non-bonded p electrons of O^{2-} ions oriented perpendicular to the bonding direction [refer to Figs. 2(c) and 1(b)].

B. Encapsulation of a single Fe atom in C12A7:O^{2-}

Here, we consider a single Fe atom occupying an empty cage in C12A7:O^{2-}. Figure 3(a) shows the optimized cage containing the Fe atom. The position of the Fe atom is off from the center of the cage. This is due to the strong attraction between Fe and cage wall O^{2-} ions. This is further confirmed by the short Fe–O bond distances (2.07 and 2.43 Å). The Bader charge on Fe is +0.14 $|e|$, meaning that a small amount of electrons have been transferred from Fe to the nearest neighboring atoms in the cage. Encapsulation energy is exoergic (−2.00 eV), implying that the Fe atom is more stable inside the cage of C12A7:O^{2-} than in its isolated form. Encapsulation does not alter the Bader charges of the extra-framework oxygen ions, as reported in Table I. The resultant encapsulated structure is magnetic, and its magnetic moment is calculated to be 4.00 μ. The valence electronic configuration of Fe is d^6s^2. In the d shell, two electrons are paired, and the other four electrons are unpaired. In the resultant complex, the Fe atom retains its electronic configuration according to the

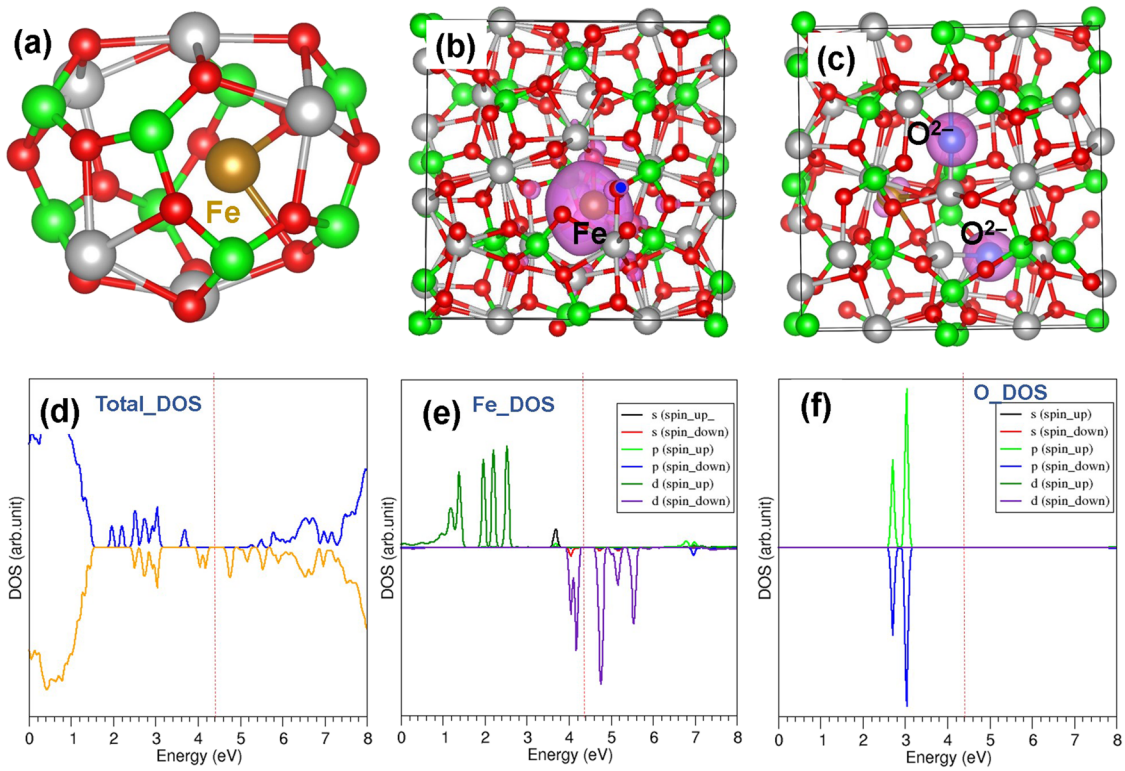

FIG. 3. (a) Optimized cage occupying Fe atom in C12A7:O^{2-}, (b) the charge density plot associated with the Fe atom, (c) the charge density plot associated with the extra-framework O^{2-} ions, (d) the total DOS plot of Fe@C12A7:O^{2-}, (e) atomic DOS of Fe, and (f) atomic DOS of extra-framework O^{2-} ions.

TABLE I. Calculated encapsulation energy, Bader charge, magnetic moment, and volume of a single Fe atom encapsulated in C12A7:O^{2-}; the available data calculated for C12A7:O^{2-} are also reported.

System	Encapsulation energy (eV)	Bader charge on Fe|e|	Bader charge on extra-framework oxygen |e|	Magnetic moment (μ)	Volume (Å^3)
Fe@C12A7:O^{2-}	−2.00	+0.14	−1.38, −1.42	4.00	1740.54
C12A7:O^{2-}	...	...	−1.40, −1.41	0.00	1738.66

Bader charge. The magnetic moment of C12A7:O^{2-} is zero, and the resultant complex has a magnetic moment of 4.00 μ. This implies that the electronic configuration of Fe is unaltered. Encapsulation introduces a very small expansion (~0.12%) in the volume.

Charge densities associated with the encapsulated Fe and the extra-framework O^{2-} ions are shown in Figs. 3(b) and 3(c), respectively. Figure 3(d) shows the total DOS plot of the encapsulated structure. Additional states appear between the top of the valence band and the Fermi energy. These states belong to the *d* states of the Fe atom, as shown in the atomic DOS of Fe [refer to Fig. 3(e)]. Atomic DOS of extra-framework O^{2-} ions are shown in Fig. 3(f). The charge density plot of extra-framework O^{2-} ions shows that charge is almost localized around the O^{2-} ions, confirming again that encapsulation does not alter the extra-framework O^{2-} ions.

C. Encapsulation of a single Fe atom in C12A7:e^-

Next, we considered the encapsulation of a single Fe atom in one of 12 empty cages in C12A7:e^-. Table II reports the encapsulation energy, Bader charge on the Fe atom, magnetic moments, and volumes calculated in the optimized structures of both C12A7:e^- and Fe@C12A7:e^-. The encapsulation energy is −1.32 eV, suggesting that the Fe atom is more stable than its isolated form. This is less negative by 0.68 eV than that calculated for single Fe atom encapsulation in C12A7:O^{2-}. This can be due to the repulsion between the *d* electrons of Fe and the extra-framework electrons in C12A7:e^-. Bader charge analysis shows that there is a charge transfer (0.86 |*e*|) from the extra-framework electrons in C12A7:e^- to Fe. The encapsulated Fe atom occupies the center of the cage (refer to Fig. 4). This is due to the electrostatic attraction between the negatively charged Fe and two cage pole Ca^{2+} ions. Zero magnetic moment is calculated for C12A7:e^-. Conversely, Fe@ C12A7:e^- exhibits a magnetic moment of 0.46 μ. As mentioned earlier, a single Fe atom has four unpaired electrons in its *d* orbital. Hence, it is expected that the net magnetic moment of Fe@ C12A7:e^- would be four. A significant reduction in the magnetic moment can be due to the pairing of four electrons of C12A7:e^- with four unpaired electrons of Fe. Figure 4(b) shows the charge density associated with the electrons. The reduction in the charge density is due to the 0.86 electrons transferred to Fe. The total DOS plot shows the extra peaks associated with the *d* states of Fe [refer to Figs. 4(c) and 4(d)]. The change in volume due to encapsulation is not significant.

TABLE II. Calculated encapsulation energy, Bader charges, magnetic moment, and volume for a single Fe atom encapsulated in C12A7:e^-; the available data calculated for C12A7:e^- are also reported.

System	Encapsulation energy (eV)	Bader charge on Fe (|e|)	Magnetic moment (μ)	Volume (Å^3)
Fe@C12A7:e^-	−1.32	−0.86	0.46	1752.60
C12A7:e^-	...	...	0.00	1752.51

D. Substitution of a single Fe atom for Al in C12A7:O^{2-}

Here, we substitute a single Fe atom on the Al site in C12A7:O^{2-}. The substitution energy is 3.02 eV, suggesting that Al–O bonds are stronger than the Fe–O bonds. This is further supported by the Bader charges of Al and Fe, bond distances, and bond angles (refer to Fig. 5 and Table III). The Bader charges of Al in C12A7:O^{2-} and Fe in Fe@C12A7:O^{2-} are +3.00 |*e*| and +1.71 |*e*|, respectively. This indicates that substitution requires energy to replace Al in the lattice. Bond distances and bond angles calculated in an AlO_4

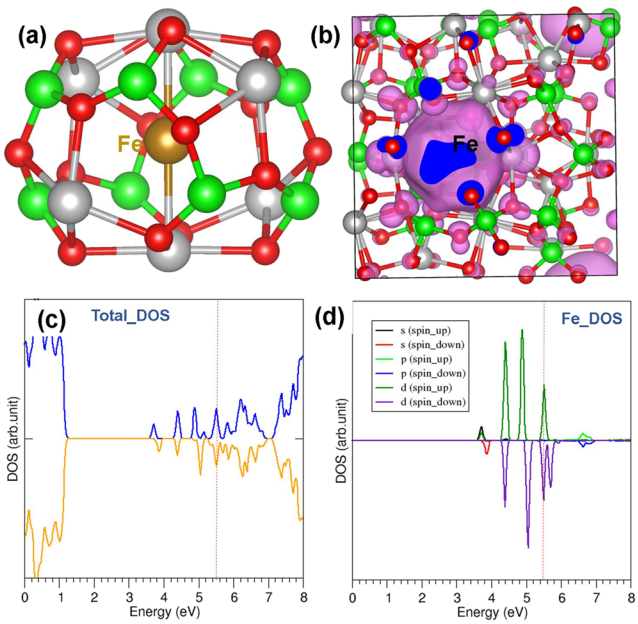

FIG. 4. (a) Optimized cage occupying Fe atom in C12A7:e^- bulk, (b) charge density associated with the electrons, (c) the total DOS plot of Fe@C12A7:e^-, and (d) atomic DOS of Fe in Fe@C12A7:e^-

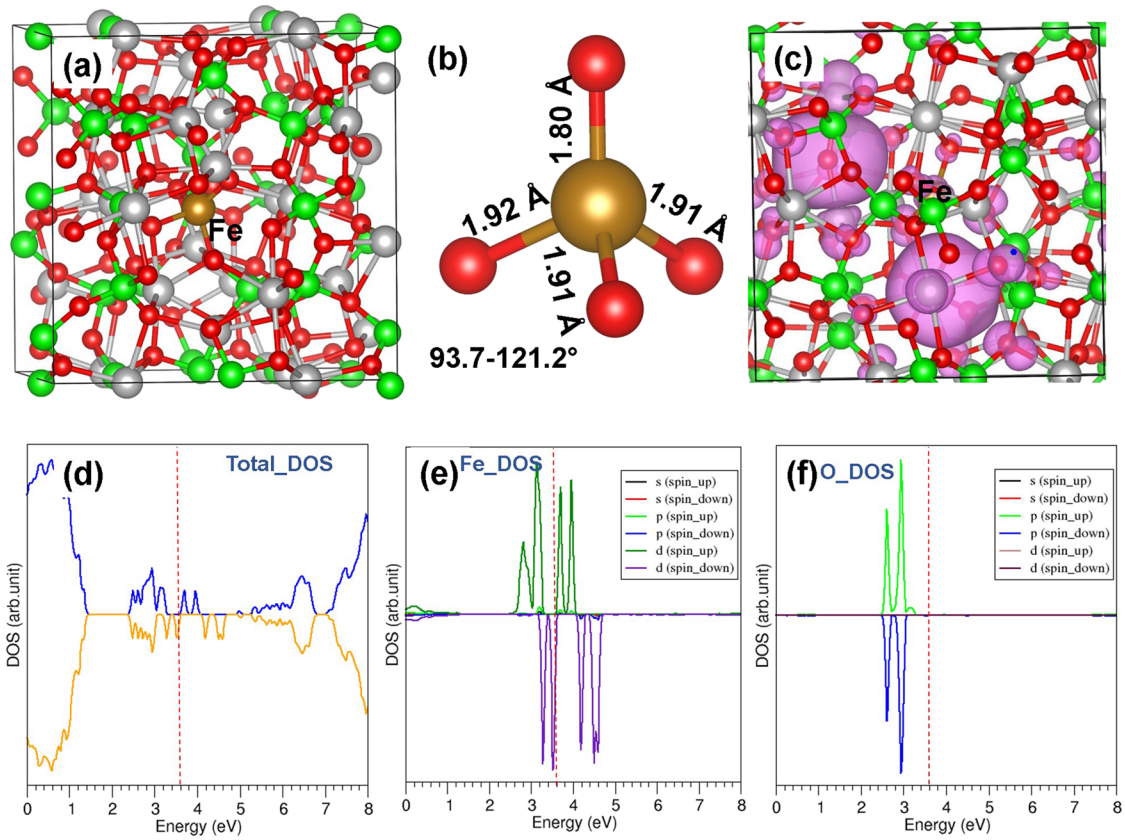

FIG. 5. (a) Relaxed structure of a single Fe atom substituted on the Al site, (b) the FeO_4 unit showing bond distances and bond angles, (c) the charge density plot associated with Fe atom and the extra-framework O^{2-} ions, (d) the total DOS plot, and (e) and (f) atomic DOS plots of Fe and extra-framework O^{2-} ions, respectively.

tetrahedral unit in C12A7:O^{2-} are 1.73–1.79 Å and 97.3°–120.3°, respectively. In a FeO_4 tetrahedral unit, bond distances are slightly longer than that calculated in the AlO_4 unit (refer to Fig. 5). Bond angles (O–Fe–O) calculated in FeO_4 also deviate slightly from the bond angles calculated (O–Al–O) in the AlO_4 unit. The Bader charges of the extra-framework O^{2-} ions show that substitution results in a negligible change (refer to Table III). The resultant substituted structure is magnetic (magnetic moment = 5.00 μ). Substitution introduced a very small expansion in the volume by ~0.3%. Figure 5 shows the relaxed configuration of the Fe atom substituted on the Al site [Fig. 5(a)], FeO_4 unit showing bond distances and bond angles [Fig. 5(b)], charge density plot associated with Fe and extra-framework O^{2-} ions [Fig. 5(c)], total DOS plot [Fig. 5(d)], and atomic DOS plots of Fe and Al [Figs. 5(e) and 5(f)].

E. Substitution of a single Fe atom for Al in C12A7:e^-

Finally, C12A7:e^- was considered for Fe substitution. The substitution energy is calculated to be 1.42 eV, inferring the stronger chemical bonding of Al^{3+} with adjacent framework O^{2-} ions than Fe^{3+} with O^{2-} ions. This is consistent with the longer Fe–O bond distances and bond angles in the FeO_4 unit [refer to Fig. 6(b)] than

TABLE III. Calculated substitution energy, Bader charges, magnetic moment, and volume for a single Fe atom substituted in C12A7:O^{2-}; the available data calculated for C12A7: O^{2-} are also reported.

System	Substitution energy (eV)	Bader charge on Fe (|e|)	Bader charge on extra-framework oxygen (|e|)	Magnetic moment (μ)	Volume (Å^3)
Fe.C12A7:O^{2-}	3.02	+1.71	−1.39, −1.40	5.00	1743.84
C12A7:O^{2-}	...	...	−1.40, −1.41	0.00	1738.66

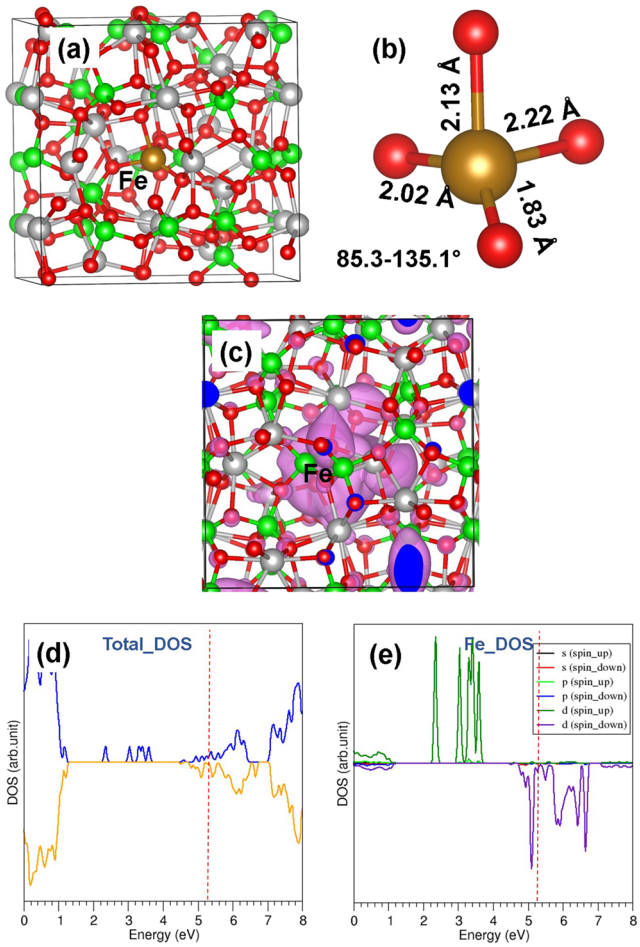

FIG. 6. (a) Relaxed structure of a single Fe atom substituted on the Al site in C12A7:e^-, (b) the FeO_4 unit showing bond distances and bond angles, (c) the charge density plot associated with the Fe atom and electrons, (d) the total DOS plot, and (e) the atomic DOS plot of Fe.

with those found in the AlO_4 unit. The Al–O bond distances and bond angles in C12A7:e^- are 1.74–1.79 Å and 99.9°–117.9°, respectively. The Bader charges on the substituted Fe and Al in C12A7 are +1.60 $|e|$ and +3.00 $|e|$, respectively, again confirming the strong bonding between the Al^{3+} ion and nearest neighboring O^{2-} ions. The resultant compound becomes magnetic, and its magnetic moment is 3.67 μ (refer to Table IV). Substitution reveals an insignificant change (~0.24%) in the volume.

Figure 6 shows the optimized structures of Fe substituted on the Al site in C12A7:e^- and the FeO_4 unit showing bond distances and bond angles, constant charge density plot associated with Fe and electrons, total DOS plot, and atomic DOS plot of Fe. Symmetrical distribution of electron density is broken upon Fe substitution, and the charge is mainly localized around the Fe atom. The total DOS plot shows that the system is still metallic, and additional peaks appear between the top of the valence band and the Fermi energy level [refer to Fig. 6(d)]. These peaks correspond to the *d* states of Fe [refer to Fig. 6(e)].

TABLE IV. Calculated substitution energy, Bader charge, magnetic moment, and volume for a single Fe atom substituted in C12A7:e^-; the available data calculated for C12A7:e^- are also reported.

System	Substitution energy (eV)	Bader charge on Fe ($\|e\|$)	Magnetic moment (μ)	Volume (Å^3)
Fe.C12A7:e^-	1.42	+1.60	3.67	1756.68
C12A7:e^-	...	...	0.00	1752.51

Current simulation results can be further expanded by making use of thermodynamic models of defects, as discussed recently by Sarlis and Skordas[35] In their models, defect formation parameters are interconnected via thermodynamical relations.

IV. CONCLUSIONS

Electronic structure calculations based on DFT were applied to examine the thermodynamical stability, charge transfer, electronic structures, and magnetic behavior of a single Fe atom encapsulated and substituted by stoichiometric and electride forms of C12A7. In both forms of C12A7, encapsulation is exoergic, and the Fe atom is more stable than its isolated form. Encapsulated structures are magnetic in contrast to their host structures, meaning that they can be of interest in the development of spintronic devices. In the electride form, the encapsulated Fe atom becomes negatively charged to provide novel chemical functionality. Substitution energies are endoergic for both forms of C12A7 due to the strong chemical bonding between Al^{3+} and framework O^{2-} ions. Substitution of Fe for Al in the electride form is thermodynamically more favorable than in its stoichiometric form by ~1.50 eV. Formation of Fe sub-bands between the Fermi energy level and the top of the valence band reveals that encapsulated or substituted C12A7 can be useful for the future applications in catalysis, optics, and electronics.

ACKNOWLEDGMENTS

Computational facilities and support were provided by the High Performance Computing Centre at Imperial College London.

The authors declare that there is no competing financial interest.

REFERENCES

[1] J. A. Imlach, L. S. Dent Glasser, and F. P. Glasser, Cem. Concr. Res. **1**, 57 (1971).
[2] S. Watauchi, I. Tanaka, K. Hayashi, M. Hirano, and H. Hosono, J. Cryst. Growth **237-239**, 801 (2002).
[3] H. Katsuro, H. Masahiro, and H. Hideo, Chem. Lett. **34**, 586 (2005).
[4] S. Matsuishi, Y. Toda, M. Miyakawa, K. Hayashi, T. Kamiya, M. Hirano, I. Tanaka, and H. Hosono, Science **301**, 626 (2003).
[5] S. W. Kim, S. Matsuishi, T. Nomura, Y. Kubota, M. Takata, K. Hayashi, T. Kamiya, M. Hirano, and H. Hosono, Nano Lett. **7**, 1138 (2007).
[6] K. Hayashi, M. Hirano, and H. Hosono, J. Phys. Chem. B **109**, 11900 (2005).
[7] M. Miyakawa, H. Kamioka, M. Hirano, T. Kamiya, P. V. Sushko, A. L. Shluger, N. Matsunami, and H. Hosono, Phys. Rev. B **73**, 205108 (2006).
[8] J. Jeevaratnam, F. P. Glasser, and L. S. D. Glasser, J. Am. Ceram. Soc. **47**, 105 (1964).
[9] G. I. Zhmoidin and A. K. Chatterjee, Cem. Concr. Res. **14**, 386 (1984).
[10] H. Hosono and Y. Abe, Inorg. Chem. **26**, 1192 (1987).

[11]M. Kitano, S. Kanbara, Y. Inoue, N. Kuganathan, P. V. Sushko, T. Yokoyama, M. Hara, and H. Hosono, Nat. Commun. **6**, 6731 (2015).
[12]Y. Toda, H. Hirayama, N. Kuganathan, A. Torrisi, P. V. Sushko, and H. Hosono, Nat. Commun. **4**, 2378 (2013).
[13]N. Kuganathan, A. Chroneos, and R. W. Grimes, Sci. Rep. **9**, 13612 (2019).
[14]N. Kuganathan, R. W. Grimes, and A. Chroneos, J. Appl. Phys. **125**, 165103 (2019).
[15]N. Kuganathan, H. Hosono, A. L. Shluger, and P. V. Sushko, J. Am. Chem. Soc. **136**, 2216 (2014).
[16]N. Kuganathan and A. Chroneos, Nanomaterials **9**, 816 (2019).
[17]M. I. Bertoni, T. O. Mason, J. E. Medvedeva, Y. Wang, A. J. Freeman, and K. R. Poeppelmeier, J. Appl. Phys. **102**, 113704 (2007).
[18]S. Matsuishi, H. Muramatsu, and H. Hosono, Chem. Lett. **43**, 1371 (2014).
[19]M. I. Bertoni, T. O. Mason, J. E. Medvedeva, A. J. Freeman, K. R. Poeppelmeier, and B. Delley, J. Appl. Phys. **97**, 103713 (2005).
[20]L. Palacios, S. Bruque, and M. A. G. Aranda, Phys. Status Solidi B **245**, 666 (2008).
[21]S. G. Ebbinghaus, H. Krause, D.-K. Lee, and J. Janek, Cryst. Growth Des. **14**, 2240 (2014).
[22]J. T. S. Irvine and A. R. West, Solid State Ionics **40-41**, 896 (1990).
[23]K. Hayashi, H. Muramatsu, S. Matsuishi, T. Kamiya, and H. Hosono, Electrochem. Solid-State Lett. **12**, J11 (2009).
[24]J. Huang, L. Valenzano, and G. Sant, Chem. Mater. **27**, 4731 (2015).
[25]C. Ruttanapun, P. Srepusharawoot, and S. Maensiri, Chin. J. Phys. **56**, 252 (2018).
[26]G. Kresse and J. Furthmüller, Phys. Rev. B **54**, 11169 (1996).
[27]G. Kresse and D. Joubert, Phys. Rev. B **59**, 1758 (1999).
[28]P. E. Blöchl, Phys. Rev. B **50**, 17953 (1994).
[29]J. P. Perdew, K. Burke, and M. Ernzerhof, Phys. Rev. Lett. **77**, 3865 (1996).
[30]H. J. Monkhorst and J. D. Pack, Phys. Rev. B **13**, 5188 (1976).
[31]W. H. Press, S. A. Teukolsky, W. T. Vetterling, and B. P. Flannery, *Numerical Recipes in C: The Art of Scientific Computing*, 2nd ed. (Cambridge University Press, 1992).
[32]S. Grimme, J. Antony, S. Ehrlich, and H. Krieg, J. Chem. Phys. **132**, 154104 (2010).
[33]G. Henkelman, A. Arnaldsson, and H. Jónsson, Comput. Mater. Sci. **36**, 354 (2006).
[34]P. V. Sushko, A. L. Shluger, Y. Toda, M. Hirano, and H. Hosono, Proc. R. Soc. A **467**, 2066 (2011).
[35]N. V. Sarlis and E. S. Skordas, Solid State Ionics **335**, 82 (2019).